REPORT DOCUMENTATION PAGE

Form Approved
OMB No. 0704-0188

1. REPORT DATE *(DD-MM-YYYY)*	2. REPORT TYPE	3. DATES COVERED *(From - To)*
APR 09	Conference Paper Postprint	Jun 08 – Jul 08

4. TITLE AND SUBTITLE

CURVATURE NONLINEARITY MEASURE AND FILTER DIVERGENCE DETECTOR FOR NONLINEAR TRACKING PROBLEMS

5a. CONTRACT NUMBER
In-House

5b. GRANT NUMBER

5c. PROGRAM ELEMENT NUMBER
62702F

6. AUTHOR(S)
Ruixin Niu, Pramod K. Varshney, Mark Alford, Adnan Bubalo, Eric Jones and Maria Scalzo

5d. PROJECT NUMBER
459E

5e. TASK NUMBER
TE

5f. WORK UNIT NUMBER
NT

7. PERFORMING ORGANIZATION NAME(S) AND ADDRESS(ES)

AFRL/RIEA
525 Brooks Road
Rome NY 13441-4505

8. PERFORMING ORGANIZATION REPORT NUMBER

9. SPONSORING/MONITORING AGENCY NAME(S) AND ADDRESS(ES)

AFRL/RIEA
525 Brooks Road
Rome NY 13441-4505

10. SPONSOR/MONITOR'S ACRONYM(S)

11. SPONSORING/MONITORING AGENCY REPORT NUMBER
AFRL-RI-RS-TP-2009-1

12. DISTRIBUTION AVAILABILITY STATEMENT
Approved for Public Release; Distribution Unlimited. PA# WPAFB 08-0464

13. SUPPLEMENTARY NOTES
Paper presented at the Information Fusion 2008 International Conference, Jun 30-Jul 3 in Cologne, Germany. One or more of the authors is a U.S. Government employee working within the scope of their Government job; therefore, the U.S. Government is joint owner of the work and has the right to copy, distribute and use the work.

14. ABSTRACT
Experimental results show that for a weekly nonlinear tracking problem, the extended Kalman filter and the unscented Kalman filter are good choices, while a particle filter should be used for problems with strong nonlinearity. To quantitatively determine the nonlinearity of a nonlinear tracking problem, we propose two types of measures: one is the differential geometry curvature measure and the other is based on the normalized innovation squared (NIS) of the Kalman filter. Simulation results show that both measures can effectively quantify the nonlinearity of the problem. The NIS is capable of detecting the filter divergence online. The curvature measure is more suitable for quantifying the nonlinearity of a tracking problem as determined via simulations.

15. SUBJECT TERMS
Tracking, extended Kalman filter, unscented Kalman filter, particle filter, nonlinearity measures

16. SECURITY CLASSIFICATION OF:			17. LIMITATION OF ABSTRACT	18. NUMBER OF PAGES	19a. NAME OF RESPONSIBLE PERSON
a. REPORT	b. ABSTRACT	c. THIS PAGE			Mark Alford
U	U	U	UU	9	19b. TELEPONE NUMBER (*Include area code*) N/A

Curvature Nonlinearity Measure and Filter Divergence Detector for Nonlinear Tracking Problems

Ruixin Niu and Pramod K. Varshney
Depart. of Electrical Engineering & Computer Science
Syracuse University
Syracuse, New York, 13244, U.S.A.
rniu@ecs.syr.edu

Mark Alford, Adnan Bubalo, Eric Jones, and Maria Scalzo
Air Force Research Laboratory/RIEA
Rome, New York 13441, U.S.A
Mark.Alford@rl.af.mil

Abstract – Several nonlinear filtering techniques are investigated for nonlinear tracking problems. Experimental results show that for a weakly nonlinear tracking problem, the extended Kalman filter and the unscented Kalman filter are good choices, while a particle filter should be used for problems with strong nonlinearity. To quantitatively determine the nonlinearity of a nonlinear tracking problem, we propose two types of measures: one is the differential geometry curvature measure and the other is based on the normalized innovation squared (NIS) of the Kalman filter. Simulation results show that both measures can effectively quantify the nonlinearity of the problem. The NIS is capable of detecting the filter divergence online. The curvature measure is more suitable for quantifying the nonlinearity of a tracking problem as determined via simulations.

Keywords: Tracking, extended Kalman filter, unscented Kalman filter, particle filter, nonlinearity measures.

1 Introduction

For nonlinear target tracking problems with nonlinear dynamics or nonlinear measurements, there exist many nonlinear filtering techniques. A comprehensive tutorial of these nonlinear techniques is given in [1]. In this paper, we investigate several of the most popular nonlinear filtering techniques, including the extended Kalman filter (EKF) [2], the unscented Kalman filter (UKF) [3] and the particle filter (PF) [4-5]. Being parametric filtering methods based on the classical Kalman filter framework, the EKF and the UKF incur only a modest amount of computational cost and lead to near-optimal performances in problems with weak nonlinearity. However, in many highly nonlinear problems, the EKF or the UKF may diverge, as shown later in this paper. The PF, a simulation-based nonparametric algorithm, has better performances than the EKF and the UKF in these difficult highly nonlinear cases. But its implementation requires a significantly larger amount of computation.

Considering the advantages and disadvantages of these filters, naturally we can employ different filtering algorithms for problems with different degrees of nonlinearity. In this paper, we study two types of nonlinearity measures to quantitatively determine the nonlinearity of a nonlinear problem. The first measure is based on the curvature measure [6], which compares the magnitude of the second-order term with that of the first-order term in a Taylor series expansion of the nonlinear problem. Recently, the curvature measures have been adopted in indicating the nonlinearity for trajectory estimation problems [7-9]. Here, we use them to determine the nonlinearity in the tracking problem. We also propose the normalized innovation squared (NIS) [2] of the Kalman filter, as a measure of nonlinearity and of filter divergence.

In Section 2, a brief introduction to the three nonlinear tracking algorithms is provided. Tracking examples with strong and weak nonlinearities to illustrate the necessity of nonlinearity measures are presented in Section 3. The curvature nonlinearity measure and the divergence detector based on Kalman filter's innovation are proposed in Section 4. There, the effectiveness of these two measures is verified by simulation results. Conclusions are drawn in Section 5.

2 Nonlinear filtering techniques

For a target tracking problem with nonlinear target motion model and/or nonlinear measurements, one of the most popular filtering techniques is the EKF, which is a minimum mean square error (MMSE) estimator based on the Taylor series expansion of the nonlinear dynamics or the nonlinear measurement [2]. It is very easy to implement and requires only modest amount of computational power.

In the first-order EKF the state distribution is approximated by a Gaussian random variable which is then propagated analytically through the first-order linearization of the nonlinear system or nonlinear measurement. Therefore, it can be viewed as providing ``first-order" approximations to the optimal terms. These approximations, however, can introduce large errors in the true posterior mean and covariance of the nonlinearly

transformed (Gaussian) random variable, which may lead to sub-optimal performance and sometimes divergence of the filter, especially in strongly nonlinear estimation problems.

The UKF addresses some approximation issues of the first-order EKF. In a UKF, The state distribution is again represented by a Gaussian random variable, but is now specified using a minimal set of carefully chosen sample points. These sample points completely capture the true mean and covariance of the Gaussian random variable, and when propagated through the true non-linear system, capture the posterior mean and covariance accurately to the 3rd order (Taylor series expansion). For details and the implementation of the UKF, the readers are referred to [3].

Another very popular strategy for estimating the state of a nonlinear system as a set of observations becomes available online is to use sequential Monte-Carlo methods, also known as the particle filter (PF). These methods allow for a complete representation of the posterior probability density function (pdf) of the states, so that any statistical estimates, such as the mean, mode, variance and kurtosis can be easily computed. They can, therefore, deal with any nonlinearity or probability distributions [5]. The basic idea of the particle filter begins with using a set of particles and their associated weights to approximate the state posterior pdf. These particles are propagated from one time to the next according to the target motion model, and their weights are updated based on the incoming measurements. It has been shown in [5] that under mild conditions, the approximation of the density function converges to the true posterior state probability density function almost surely as the number of particles goes to infinity. In this paper, we adopt a very simple and popular version of the PF, the sequential importance resampling (SIR) particle filtering algorithm [5].

3 Motivating examples

3.1 Target and measurement models

We assume that the target motion is modeled as follows

$$\mathbf{x}_k = \mathbf{F}\mathbf{x}_{k-1} + \mathbf{v}_k \qquad (1)$$

where $\mathbf{x}_k = [\xi_k \ \dot{\xi}_k \ \eta_k \ \dot{\eta}_k]'$ is the target state at time k, consisting of positions and velocities along ξ and η axes in a two-dimensional Cartesian coordinate system. $\mathbf{F}$ is the state transition matrix

$$\mathbf{F} = \begin{bmatrix} 1 & T & 0 & 0 \\ 0 & 1 & 0 & 0 \\ 0 & 0 & 1 & T \\ 0 & 0 & 0 & 1 \end{bmatrix} \qquad (2)$$

in which T is the time interval between two adjacent samples. $\mathbf{v}_k$ denotes the zero-mean white Gaussian noise with covariance matrix $\mathbf{Q}$

$$\mathbf{Q} = q\begin{bmatrix} T^3/3 & T^2/2 & 0 & 0 \\ T^2/2 & T & 0 & 0 \\ 0 & 0 & T^3/3 & T^2/2 \\ 0 & 0 & T^2/2 & T \end{bmatrix} \qquad (3)$$

where q is a scalar. For a radar that reports range-bearing measurements, the measurement model can be mathematically written as

$$\mathbf{z}_k = \mathbf{h}(\mathbf{x}_k) + \mathbf{w}_k \qquad (4)$$

where $\mathbf{z}_k$ is the radar measurement,

$$\mathbf{h}(\mathbf{x}_k) = \begin{bmatrix} \sqrt{(\xi_k - \xi_s)^2 + (\eta_k - \eta_s)^2} \\ \tan^{-1}\left[(\eta_k - \eta_s)/(\xi_k - \xi_s)\right] \end{bmatrix} \qquad (5)$$

(ξ_k, η_k) is the target position at time *k*, and (ξ_s, η_s) is the position of the radar. $\mathbf{w}_k$ denotes the measurement noise, which is Gaussian with zero mean and covariance matrix **R**. As we can see, the motion model is linear and Gaussian. But the measurements are nonlinear functions of the target state.

Note that for the EKF, Jacobian of measurement is given by

$$\mathbf{J}_k = \begin{bmatrix} \dfrac{\Delta\xi_k}{\sqrt{\Delta\xi_k^{\ 2} + \Delta\eta_k^{\ 2}}} & 0 & \dfrac{\Delta\eta_k}{\sqrt{\Delta\xi_k^{\ 2} + \Delta\eta_k^{\ 2}}} & 0 \\ \dfrac{-\Delta\eta_{kj}}{\Delta\xi_k^{\ 2} + \Delta\eta_k^{\ 2}} & 0 & \dfrac{\Delta\xi_{kj}}{\Delta\xi_k^{\ 2} + \Delta\eta_k^{\ 2}} & 0 \end{bmatrix} \qquad (6)$$

where $\Delta\xi_k = \hat{\xi}_{k|k-1} - \xi_s$ and $\Delta\eta_k = \hat{\eta}_{k|k-1} - \eta_s$.

3.2 A single radar with strong nonlinearity

In this experiment, we assume that there is a single radar sensor that is tracking the target. An example for the target trajectory has been shown in Fig. 1.

First, we investigate a case with highly nonlinear measurements. We assume that the range measurements

are very accurate, with a range error standard deviation (s.d.) of 10 m, and the bearing measurements are relatively coarse, with a bearing error s.d. of 3°. Given the geometry in Fig. 1, it can be shown that the uncertainty region of the target position based on the range and the bearing measurements is part of a thin ring with its span proportional to the s.d. of the bearing measurement.

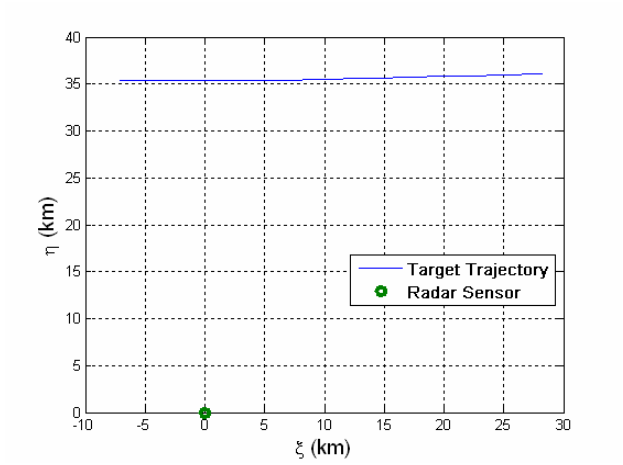

Fig. 1 Geometry of the target trajectory and the radar sensor.

In the experiment, the PF uses 2×10^4 particles. The root mean square errors (RMSEs) are obtained by taking an average over 100 Monte-Carlo simulation runs. In Fig. 2, the RMSEs of position estimates are shown. Since the RMSEs of velocity estimates exhibit similar behaviors to those of position estimates, they are not shown to save space. From Fig. 2, it is clear that the EKF's averaged RMSEs are much higher than those of the other two algorithms. This is because in some Monte-Carlo runs, the EKF diverges. Since an unscented transform has been used in the UKF, the UKF provides significant improvement over the EKF. The PF outperforms the UKF, at the cost of much more computational complexity.

3.3 A single radar with weak nonlinearity

Second, we investigate a case with less nonlinearity in the measurements. We assume that the range measurement error has a s.d. of 100 m, and the bearing measurement error has a s.d. of 1°. As shown in Fig. 3, all the three algorithms have performances close to each other. This implies that for a recursive estimation problem with weak nonlinearity, the EKF or the UKF should be used to save the computational cost, while at the same time to achieve the same performances as that of the PF.

3.4 Computational complexities

To quantitatively compare the complexities of different algorithms, the average number of floating point operations per iteration for each algorithm is listed in Table I. Note that in the PF, 2×10^4 particles have been used. As we can see, the computational costs for the PF are much higher than those of the EKF and the UKF.

Table I. Average number of floating point operations per iteration for different algorithms

EKF	UKF	PF
1138	3161	2146055

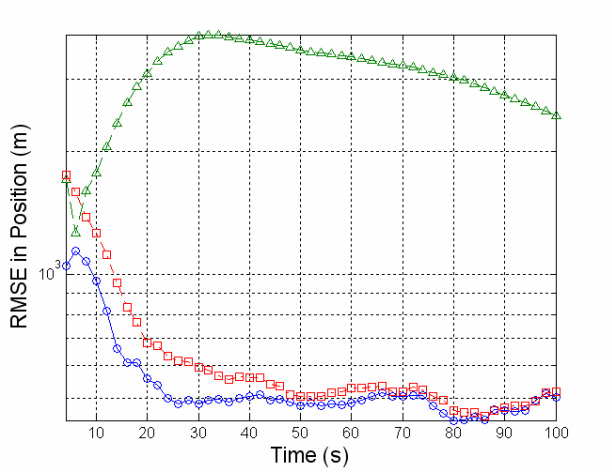

Fig. 2 RMSEs in position estimates by different tracking algorithms. Triangle: EKF. Square: UKF. Circle: PF.

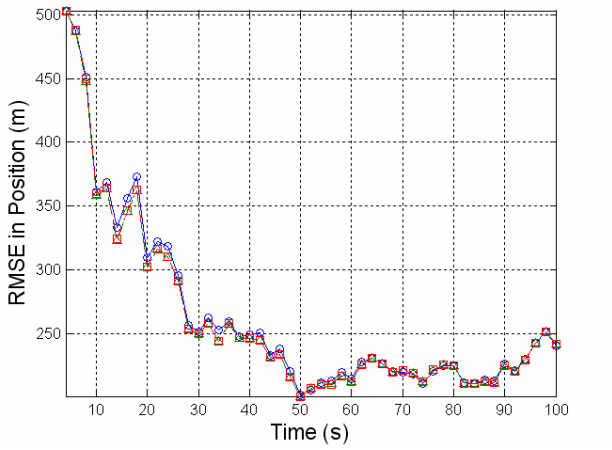

Fig. 3 RMSEs in position estimates by different tracking algorithms. Triangle: EKF. Square: UKF. Circle: PF.

4 Nonlinearity measures

From the examples in the last section, we can see that under different circumstances, it is desirable to apply different filtering algorithms. For a tracking problem with

weak nonlinearity, the EKF and the UKF are good choices, since they provide near-optimal tracking performances, while at the same time have much less computation complexity than the PF. However, in a highly nonlinear problem, the PF should be used, since the EKF and the UKF are prone to divergence in such a problem. As a result, it is important to develop a metric to gauge the nonlinearity of the estimation problem. For the tracking problem with linear dynamic model and nonlinear measurement model, the nonlinearity is brought by the nonlinear measurements. We propose the parameter-effects curvature and intrinsic curvature, similar to those used in [7], to measure the nonlinearity in the measurements. However, we also observe that the curvature measures can not provide a direct and timely indication of the divergence of the EKF or the UKF. To detect the divergence of a filter in a timely manner, we also develop a Chi-square detector based on the innovation of the Kalman filter, which checks the consistency of the filter, and detects the filter divergence when it occurs.

4.1 Curvature nonlinearity measures

We try to measure the nonlinearity in the measurements using curvature measures [6], as proposed in [7]. In [7], the measures have been used in trajectory estimation problems. Here we apply them for measuring and detecting the nonlinearity in target tracking problems.

The nonlinear measurement model (4) can be rewritten as

$$\mathbf{z}_k = \mathbf{h}(\mathbf{p}_k) + \mathbf{w}_k \qquad (7)$$

where $\mathbf{p}_k = [\xi_k \ \eta_k]'$ is the target's coordinates at time k, since $\mathbf{z}_k$ is not a function of the target's velocity at time k. In a EKF, the nonlinear measurement is approximated by the first order Taylor series expansion of $\mathbf{h}(\mathbf{p}_k)$ about the predicted target position $\hat{\mathbf{p}}_{k|k-1}$:

$$\mathbf{h}(\mathbf{p}_k) \approx \mathbf{h}(\hat{\mathbf{p}}_{k|k-1}) + \dot{\mathbf{H}}_k(\hat{\mathbf{p}}_{k|k-1})(\mathbf{p}_k - \hat{\mathbf{p}}_{k|k-1}) \qquad (8)$$

where

$$\dot{\mathbf{H}}_k(\hat{\mathbf{p}}_{k|k-1}) = \left.\frac{\partial \mathbf{h}(\mathbf{p}_k)}{\partial \mathbf{p}_k}\right|_{\mathbf{p}_k=\hat{\mathbf{p}}_{k|k-1}}, \quad \dot{\mathbf{H}}_k(\hat{\mathbf{p}}_{k|k-1}) \in R^{n_z \times n_p} \qquad (9)$$

where n_z and n_p are the dimensions of the measurement and the target position, respectively. The first-order EKF uses the linear approximation by ignoring the higher order terms in the Taylor series expansion. The linear approximation in the EKF is valid only if the measurement function is relatively flat near $\hat{\mathbf{p}}_{k|k-1}$ and the hence the tangent plane approximation in (8) is valid. Taking the Taylor series expansion of (7) up to the second order, we have

$$\begin{aligned}\mathbf{h}(\mathbf{p}_k) \approx{}& \mathbf{h}(\hat{\mathbf{p}}_{k|k-1}) + \dot{\mathbf{H}}_k(\hat{\mathbf{p}}_{k|k-1})(\mathbf{p}_k - \hat{\mathbf{p}}_{k|k-1}) \\ &+ \frac{1}{2}(\mathbf{p}_k - \hat{\mathbf{p}}_{k|k-1})'\ddot{\mathbf{H}}_k(\hat{\mathbf{p}}_{k|k-1})(\mathbf{p}_k - \hat{\mathbf{p}}_{k|k-1})\end{aligned} \qquad (10)$$

where

$$\ddot{\mathbf{h}}_{mij}(\hat{\mathbf{p}}_{k|k-1}) = \left.\frac{\partial^2 \mathbf{h}_m(\mathbf{p})}{\partial \mathbf{p}_i \partial \mathbf{p}_j}\right|_{\mathbf{p}=\hat{\mathbf{p}}_{k|k-1}}, \quad \ddot{\mathbf{H}}(\hat{\mathbf{p}}_{k|k-1}) \in R^{n_z \times n_p \times n_p}, \qquad (11)$$

$m = 1, \cdots, n_z, i, j = 1, \cdots, n_p$

According to the linear approximation (8), $\mathbf{h}(\mathbf{p}_k)$ lies in the plane tangent to the measurement surface at the point $\hat{\mathbf{p}}_{k|k-1}$. Therefore, the linearization in the measurement model is equivalent to approximating the measurement surface by the tangent plane at $\hat{\mathbf{p}}_{k|k-1}$. The tangent plane is a good approximation to the measurement surface if the norm of the quadratic term $\left\|(\mathbf{p}_k - \hat{\mathbf{p}}_{k|k-1})'\ddot{\mathbf{H}}_k(\hat{\mathbf{p}}_{k|k-1})(\mathbf{p}_k - \hat{\mathbf{p}}_{k|k-1})\right\|$ is negligible compared with the norm of the linear term $\left\|\dot{\mathbf{H}}_k(\hat{\mathbf{p}}_{k|k-1})(\mathbf{p}_k - \hat{\mathbf{p}}_{k|k-1})\right\|$. It is useful to decompose the quadratic term on the right hand side of (10) into components in the tangent plane and orthogonal to the tangent plane.

In order to define the curvature measures of nonlinearity, velocity vectors and acceleration vectors [6] are introduced, which form the Jacobian and Hessian, respectively. The $n_z \times 1$ velocity vectors are defined by

$$\dot{\mathbf{h}}_{ki}(\hat{\mathbf{p}}_{k|k-1}) = \left[\left.\frac{\partial \mathbf{h}_1(\mathbf{p}_k)}{\partial \mathbf{p}_{ki}}\right|_{\mathbf{p}_k=\hat{\mathbf{p}}_{k|k-1}} \cdots \left.\frac{\partial \mathbf{h}_{n_z}(\mathbf{p}_k)}{\partial \mathbf{p}_{ki}}\right|_{\mathbf{p}_k=\hat{\mathbf{p}}_{k|k-1}}\right]' \qquad (12)$$

$i = 1, 2, \cdots n_p$

and

$$\dot{\mathbf{H}}_k(\hat{\mathbf{p}}_{k|k-1}) = \left[\dot{\mathbf{h}}_{k1}(\hat{\mathbf{p}}_{k|k-1}) \cdots \dot{\mathbf{h}}_{kn_p}(\hat{\mathbf{p}}_{k|k-1})\right] \qquad (13)$$

The $n_z \times 1$ symmetric acceleration vectors are defined by

$$\ddot{\mathbf{h}}_{ij}(\hat{\mathbf{p}}_{k|k-1}) = \left.\frac{\partial^2 \mathbf{h}(\mathbf{p_k})}{\partial \mathbf{p}_i \partial \mathbf{p}_j}\right|_{\mathbf{p}=\hat{\mathbf{p}}_{k|k-1}}, \quad \ddot{\mathbf{h}}_{ij}(\hat{\mathbf{p}}_{k|k-1}) \in R^{n_z \times 1} \qquad (14)$$

$i, j = 1, \cdots, n_p$

The acceleration vectors are decomposed into components in the tangent plane and orthogonal to the tangent plane. Let $\ddot{\mathbf{H}}_m(\mathbf{p}_{k|k-1}) \in R^{n_p \times n_p}$ denote the *m*th face of the acceleration array

$$\ddot{\mathbf{H}}_m(\hat{\mathbf{p}}_{k|k-1}) = \begin{bmatrix} \ddot{\mathbf{h}}_{m11}(\hat{\mathbf{p}}_{k|k-1}) & \cdots & \ddot{\mathbf{h}}_{m1n_p}(\hat{\mathbf{p}}_{k|k-1}) \\ \cdots & \cdots & \cdots \\ \ddot{\mathbf{h}}_{mn_p1}(\hat{\mathbf{p}}_{k|k-1}) & \cdots & \ddot{\mathbf{h}}_{mn_pn_p}(\hat{\mathbf{p}}_{k|k-1}) \end{bmatrix} \quad (15)$$
$$m = 1, 2, \cdots n_z$$

The projection matrix $\mathbf{P}_T$ which projects an $n_z \times 1$ vector into the tangent plane is defined by

$$\mathbf{P}_T = \dot{\mathbf{H}}_k(\hat{\mathbf{p}}_{k|k-1})\left[\dot{\mathbf{H}}_\mathbf{k}'(\hat{\mathbf{p}}_{k|k-1})\dot{\mathbf{H}}_k(\hat{\mathbf{p}}_{k|k-1})\right]^{-1}\dot{\mathbf{H}}_k'(\hat{\mathbf{p}}_{k|k-1}) \quad (16)$$

Therefore, we can decompose an acceleration vector into components tangent and orthogonal to the tangent plane. Let $\ddot{\mathbf{h}}_{ij}^T(\hat{\mathbf{p}}_{k|k-1})$ and $\ddot{\mathbf{h}}_{ij}^N(\hat{\mathbf{p}}_{k|k-1})$ denote the tangential and orthogonal components of the acceleration vector $\ddot{\mathbf{h}}_{ij}(\hat{\mathbf{p}}_{k|k-1})$, respectively. Then

$$\begin{aligned} \ddot{\mathbf{h}}_{ij}^T(\hat{\mathbf{p}}_{k|k-1}) &= \mathbf{P}_T\ddot{h}_{ij}(\hat{\mathbf{p}}_{k|k-1}) \\ \ddot{\mathbf{h}}_{ij}^N(\hat{\mathbf{p}}_{k|k-1}) &= (\mathbf{I}-\mathbf{P}_T)\ddot{\mathbf{h}}_{ij}(\hat{\mathbf{p}}_{k|k-1}) \\ \ddot{\mathbf{h}}_{ij}(\hat{\mathbf{p}}_{k|k-1}) &= \ddot{\mathbf{h}}_{ij}^T(\hat{\mathbf{p}}_{k|k-1}) + \ddot{\mathbf{h}}_{ij}^N(\hat{\mathbf{p}}_{k|k-1}) \end{aligned} \quad (17)$$

for $i, j = 1, \cdots, n_p$. Use of (17) for the quadratic term in (10) gives

$$\left\|\boldsymbol{\delta}_k'\ddot{\mathbf{H}}(\hat{\mathbf{p}}_{k|k-1})\boldsymbol{\delta}_k\right\|^2 = \left\|\boldsymbol{\delta}_k'\ddot{\mathbf{H}}^T(\hat{\mathbf{p}}_{k|k-1})\boldsymbol{\delta}_k\right\|^2 + \left\|\boldsymbol{\delta}_k'\ddot{\mathbf{H}}^N(\hat{\mathbf{p}}_{k|k-1})\boldsymbol{\delta}_k\right\|^2 \quad (18)$$

where

$$\boldsymbol{\delta}_k = \mathbf{p}_k - \hat{\mathbf{p}}_{k|k-1} \quad (19)$$

Bates and Watts [6] define the parameter-effects curvature K_δ^T and intrinsic curvature K_δ^N as two measures of nonlinearity, which compare the quadratic term with the linear term in the direction of the vector δ_k in the parameter space. These two curvature measures are defined as

$$K_{\boldsymbol{\delta}}^T = \frac{\left\|\boldsymbol{\delta}_k'\ddot{\mathbf{H}}^T(\hat{\mathbf{p}}_{k|k-1})\boldsymbol{\delta}_k\right\|}{\left\|\dot{\mathbf{H}}(\hat{\mathbf{p}}_{k|k-1})\boldsymbol{\delta}_k\right\|^2} \quad (20)$$

$$K_{\boldsymbol{\delta}}^N = \frac{\left\|\boldsymbol{\delta}_k'\ddot{\mathbf{H}}^N(\hat{\mathbf{p}}_{k|k-1})\boldsymbol{\delta}_k\right\|}{\left\|\dot{\mathbf{H}}(\hat{\mathbf{p}}_{k|k-1})\boldsymbol{\delta}_k\right\|^2} \quad (21)$$

4.2 Chi-square detector based on innovation

To check if the EKF or UKF diverges, a very effective way is to calculate the normalized innovation squared (NIS) [2] of the EKF or UKF and compare it with a threshold. The NIS is defined as

$$NIS = [\mathbf{z}_k - \mathbf{h}(\hat{\mathbf{x}}_{k|k-1})]'\mathbf{S}_k^{-1}[\mathbf{z}_k - \mathbf{h}(\hat{\mathbf{x}}_{k|k-1})] \quad (22)$$

where $\mathbf{z}_k - \mathbf{h}(\hat{\mathbf{x}}_{k|k-1})$ is the innovation of the EKF or the UKF, and

$$\mathbf{S}_k = \mathbf{J}_k\mathbf{P}_{k|k-1}\mathbf{J}_k' + \mathbf{R} \quad (23)$$

is the covariance matrix of the innovation, which is provided by the filter. When the linear and Gaussian assumption is reasonably good, the innovation is a zero-mean Gaussian and its covariance is given by $\mathbf{S}_k$. In such a case, the NIS follows a Chi-square distribution with n_z degrees of freedom. However, when the filter diverges, the NIS will no longer follow a Chi-square distribution. Hence, we propose to check if the NIS falls into the $1-\alpha$ confidence region for a Chi-square random variable with n_z degrees of freedom, to judge if the filter diverges. Here α is a very small number, which is actually determined by the false alarm rate of the Chi-square detector.

4.3 Experimental results

4.3.1 A single radar with strong nonlinearity

In this experiment, we assume that there is a single radar sensor that is tracking the target. The geometry of the radar and the trajectory is similar to that shown in Fig. 1. First, we investigate a case with highly nonlinear measurements. We assume that the range measurements are very accurate, with a range error standard deviation (s.d.) of 10 m, and the bearing measurements are relatively coarse, with a bearing error s.d. of 4°.

For a single Monte-Carlo run, the target state estimation errors are plotted in Fig. 4 for different algorithms. It can be seen that the EKF diverges, while the PF and the UKF converges and have very similar performances.

In Fig. 5, the parameter-effects curvature defined in (20) have been plotted for the EKF and the UKF. It is clear that the maximum curvature measure for the EKF (around 100) is much greater than that of the UKF (below 1), indicating that the EKF is not working properly. However, the curvature measures can not indicate the divergence of the EKF in real time, since its peak value occurs a long time after the EKF diverges.

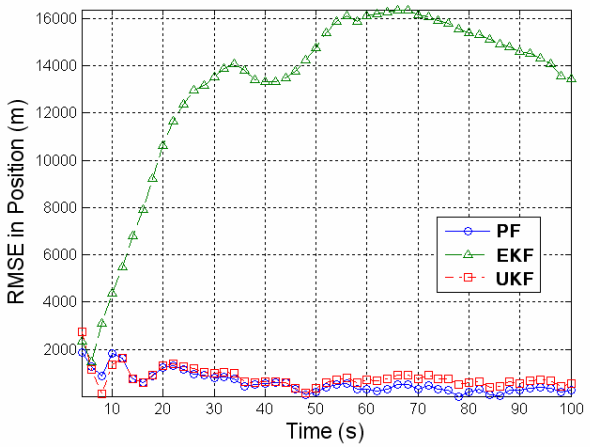

Fig. 4 RMSEs in position by different tracking algorithms.

In Fig. 6, the NISs are shown for the EKF and the UKF. It is evident that for most of the time, the NIS of the EKF is outside the one-sided 98% confidence region of the Chi-square distribution with two degrees of freedom, correctly indicating the EKF is diverging. On the contrary, the NIS for the UKF is inside the 98% confidence region at all of the time. It is clear that the Chi-square detector based on the innovation of the Kalman filter is effective in detecting the filter divergence in real time.

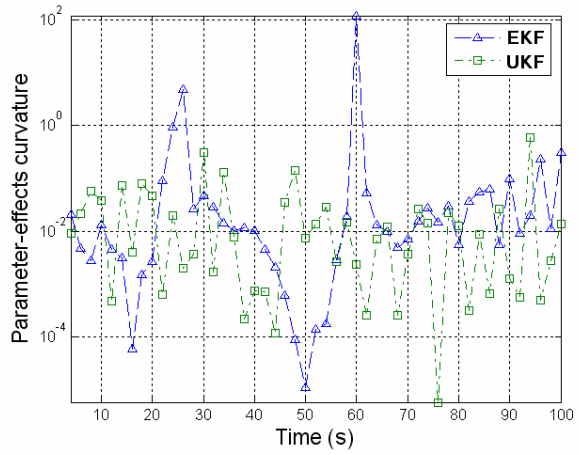

Fig. 5 Curvature measures for the EKF and the UKF.

4.3.2 A single radar with weak nonlinearity

We investigate a case with very weak nonlinearity in the measurements. We assume that the range measurement error has a s.d. of 100 m, and the bearing measurement has a s.d. of 1°. As we can see from Fig. 7, both the EKF and the UKF work well and have performances which are very close to that of the PF.

In Fig. 8, the curvature measures for the EKF and the UKF are plotted. It is clear that due to the low nonlinearity, the curvature measures are very small.

Similarly, the NISs for the EKF and the UKF are within the 98% confidence region for all the time, as illustrated in Fig. 9.

4.3.3 Two bearing sensors

In this experiment, we assume that two bearing-only sensors are used to provide positional information to the tracker. The target trajectory and the positions of the two sensors are shown in Fig. 10. Each sensor has a measurement error s.d. of 3°.

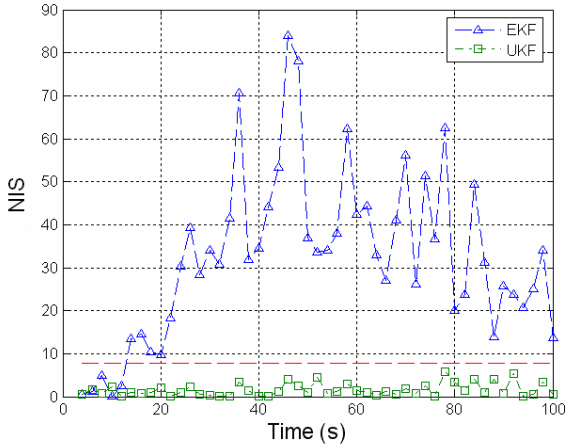

Fig. 6 NISs for the EKF and the UKF. Dashed line denotes the one-sided 98% confidence region.

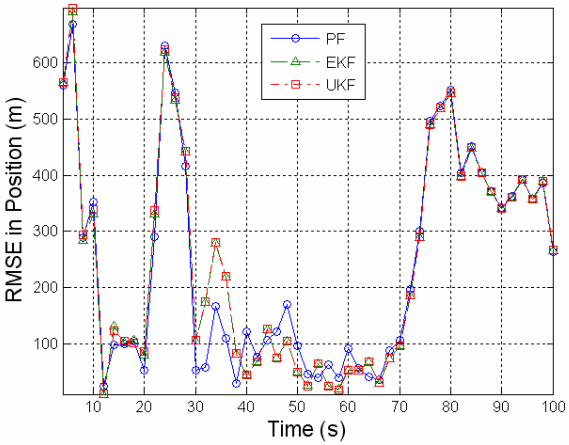

Fig. 7 Tracking performances of different tracking algorithms.

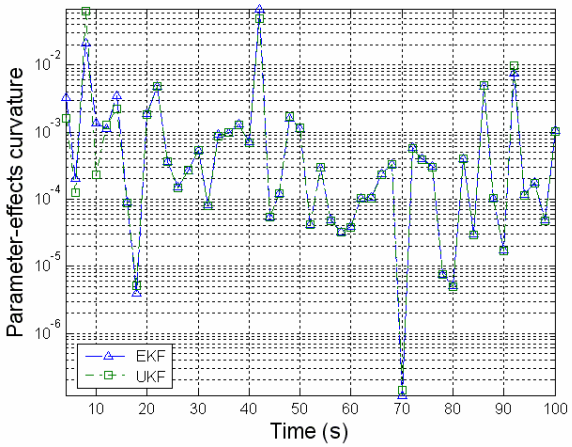

Fig. 8 Curvature measures for the EKF and the UKF.

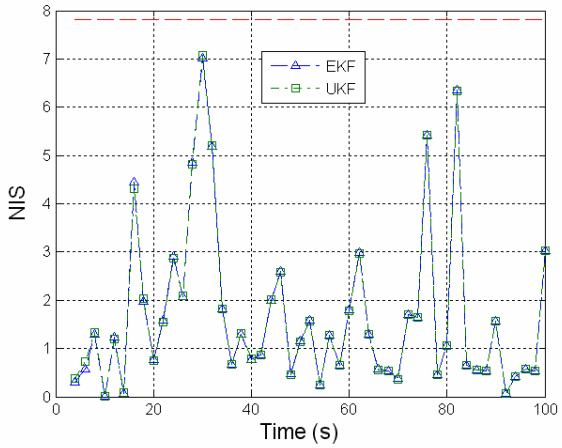

Fig. 9 NISs for the EKF and the UKF. The dashed line denotes the one-sided 98% confidence region.

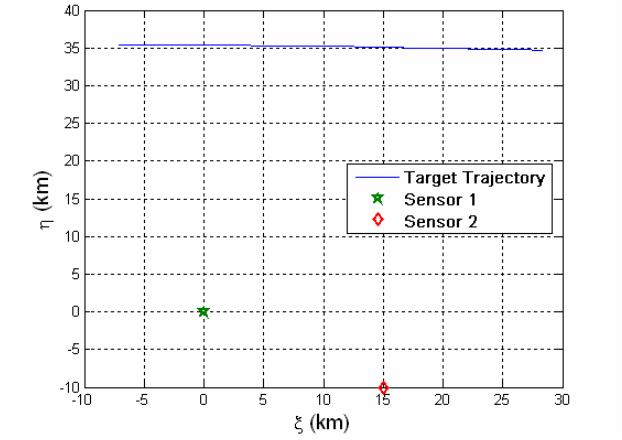

Fig. 10 Geometry of the target trajectory and the bearing sensors.

The tracking performances, the curvature measures and the NISs are plotted in Figs. 11-13, respectively. It can be seen that the UKF diverges in the first 50 seconds, during which time, its NIS falls outside the 98% confidence region. The peak values of its curvature measures are much greater than those of the EKF.

In summary, both the curvature measure and the NIS are effective measures of the nonlinearity of the nonlinear tracking problems. One problem with the curvature measure is that its evaluation requires the true value of the target position $[\xi_k \ \eta_k]'$, which is not available on-line. One possible solution is to use the updated position estimate $[\hat{\xi}_{k|k} \ \hat{\eta}_{k|k}]'$, which is generated by the filter, to replace $[\xi_k \ \eta_k]'$. This estimated value, however, is not robust, especially when the filter itself is diverging. On the other hand, one can certainly use the curvature measures offline via simulations, to evaluate the nonlinearity of a specific tracking problem, with all the pre-specified parameters.

The NIS, however, does not require the knowledge of the true $[\xi_k \ \eta_k]'$, since the innovation is simply the difference between the predicted measurement provided by the filter, and the incoming measurement. As we have observed in the experiments, the NIS is very effective in indicating the divergence of the filter, when there is significant mismatch between its estimation error and its calculated covariance matrix.

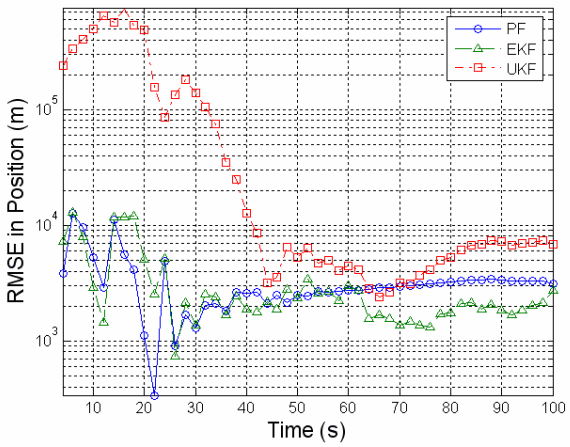

Fig. 11 Tracking performances of different tracking algorithms.

5 Conclusion

In this paper, we investigated different nonlinear filtering techniques, including the EKF, the UKF, and the PF for nonlinear target tracking problems under various scenarios. Their tracking performances were compared and their complexities were evaluated in terms of the numbers of floating point operations. It was shown that for a tracking problem with weak nonlinearity, the EKF and the UKF are near-optimal and it is not necessary to

employ the computationally expensive particle filter. However, for problems with strong nonlinearity, particle filters should be used to get reliable tracking performances.

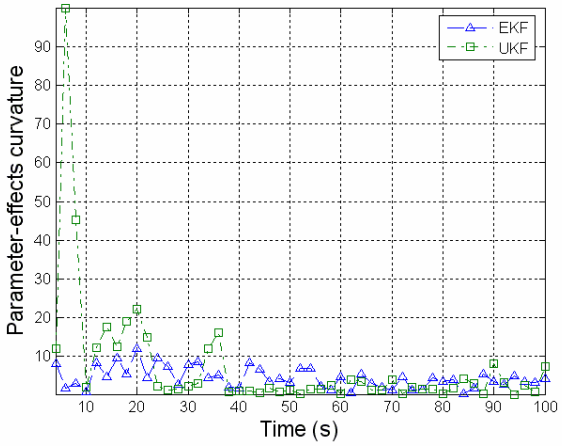

Fig. 12 Curvature measures for the EKF and the UKF over time.

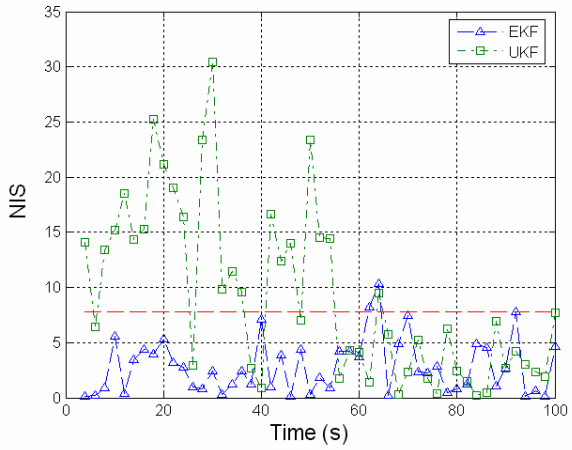

Fig. 13 NISs for the EKF and the UKF. The dashed line denotes the one-sided 98% confidence region.

To measure the nonlinearity of the tracking problem, we explored two types of measures. One type of measure is based on the curvature measures, which compares the magnitude of the second-order term with that of the first-order term in a Taylor series expansion of the nonlinear problem. The second measure calculates the normalized innovation squared (NIS) of the Kalman filter, which indicates filter divergence when it exceeds a certain threshold. Experiments show that both measures are effective in measuring the nonlinearity of the problem. The curvature measures are more suitable for the offline operation while the NIS can detect filter divergence online in real time.

Acknowledgment

This work was supported by the USAF AFRL under Contract FA8750-06-C-0001. We are grateful to Mark Kozak and Tim Bumpus for valuable discussions during the course of this work.

References

[1] Z. Chen, ``Bayesian filtering: From Kalman filters to particle filters, and beyond'', *Adaptive Syst. Lab., McMaster Univ., Hamilton, ON, Canada. [Online], http://users.isr.ist.utl.pt/~jpg/tfc0607/chen_bayesian.pdf*, 2003.

[2] Y. Bar-Shalom, X.R. Li, and T. Kirubarajan, *Estimation with Applications to Tracking and Navigation*, New York: Wiley, 2001.

[3] S.J. Julier, J.K. Uhlmann, ``A New Extension of the Kalman Filter to Nonlinear Systems'', *Int. Symp. Aerospace/Defense Sensing, Simul. and Controls*, Orlando, FL,1997.

[4] N. Gordon, D. Salmond, and A. F. M. Smith, "Novel approach to nonlinear and non-Gaussian Bayesian state estimation," in *Proceedings IEE-F*, vol. 140, pp. 107--113, 1993.

[5] A. Doucet, N. de Freitas, and N. Gordon, *Sequential Monte Carlo Methods in Practice. Statistics for Engineering and Information Science*. New York: Springer-Verlag, 2001.

[6] D.M. Bates and D.G. Watts, *Nonlinear Regression Analysis and its Applications*, John Wiley, 1988.

[7] M. Mallick, B. F. La Scala and S. Arulampalam ``Differential Geometry Measures of Nonlinearity for the Bearing-Only Tracking Problem'', *SPIE Conference on Signal Processing, Sensor Fusion and Target Recognition*, Vol 5809, Orlando, FL, USA, March 2005.

[8] M. Mallick, and B.F. La Scala, ``Differential Geometry Measures of Nonlinearity for Ground Moving Target Indicator (GMTI) Filtering'', *Proceedings of the 8th International conference on Information Fusion*, pp. 219- 226, July 2005.

[9] M. Mallick and B. F. La Scala, ``Differential Geometry Measures of Nonlinearity for the Video Tracking Problem'', *SPIE Conference on Signal Processing, Sensor Fusion and Target Recognition*, Vol 6235, Orlando, FL, USA, April 2006.